# Neutron-induced fission cross section of $^{237}U$

J. H. McNally, J. W. Barnes, B. J. Dropesky, P. A. Seeger, and K. Wolfsberg
*Los Alamos Scientific Laboratory, University of California, Los Alamos, New Mexico 87544*
(Received 5 March 1973)

An 18.1-$\mu$g sample of $^{237}U$ (half-life $6.70 \pm 0.02$ day) was prepared and exposed to a neutron beam from the underground nuclear explosion Pommard. The neutron-induced fission cross section was measured from 43 to 1000 eV and from 0.1 to 2 MeV. A resonance analysis was attempted from 43 to 220 eV; resonance areas are reported. Both $0^+$ and $1^+$ seem to be present, with average spacing 3.5 eV. The cross section at 1 MeV is $1.0 \pm 0.1$ b; from 300–1000 eV, the cross section is 30% of that for $^{239}Pu$.

[NUCLEAR REACTIONS, FISSION $^{237}U(n,f)$, $E = 43$–1000 eV, $E = 0.1$–2 MeV; measured $\sigma(E)$. Nuclear explosion.]

## I. INTRODUCTION

The use of an underground nuclear explosion as an intense neutron source for time-of-flight cross-section measurements has been described in previous publications and reports.[1-4] The advantages of this method over more customary laboratory sources lie in the extreme intensity of the neutron beam. A rough rule is that 1 g of neutrons is released for each 17-TJ yield of the nuclear device. For the Pommard event of March 1968, the yield was 5.5 TJ, the moderator intercepted about 10%. and the solid angle of the collimator orifice was $10^{-7}$ of the sphere; thus, approximately $10^{15}$ neutrons passed through the target array in a single pulse. The width of the unmoderated pulse was about 0.1 $\mu$sec. Peak instantaneous currents measured were $1.5 \times 10^{18}$ $n$/sec at 1 MeV and $6 \times 10^{15}$ $n$/sec at 130 eV (the thermal peak from the moderator).

Three advantages of the high intensity are: (1) Detectable reaction rates may be obtained from very small samples. (2) Targets with short half-lives will not decay during the experiment. (3) Backgrounds and detector damage from highly radioactive targets are negligible. These features made possible the measurement of $^{237}U$, which could not be done by any other present-day technique.

## II. TARGET PREPARATION AND COMPOSITION

The short half-life of $^{237}U$ and the rigid timing of the Pommard event necessitated a smooth scheduling of events leading to the placement of the $^{237}U$ target on the experiment tower. These events involved production of the $^{237}U$ by neutron irradiation of $^{236}U$ in the high flux isotopes reactor (HFIR) facility at Oak Ridge National Laboratory (ORNL), air shipment directly to Los Alamos Scientific Laboratory (LASL) for chemical purification of the uranium and isotopic separation of the $^{237}U$, and then air shipment of the $^{237}U$ target to the Nevada Test Site.

### A. $^{236}U$ irradiation

The reactor target material (obtained from ORNL) was 42 mg of uranium, as $U_3O_8$, which had the following isotopic composition: $^{235}U$, 0.16%; $^{236}U$, 99.62%; and $^{238}U$, 0.22%. This material was incorporated into the interior of a solid aluminum "rabbit," which was then irradiated for 22 days in the HFIR in a nominal flux of $2.2 \times 10^{15}$ thermal neutrons/cm$^2$ sec and of $1.0 \times 10^{14}$ resonance neutrons/(cm$^2$ sec unit lethargy). Approximately 1.9% of the $^{236}U$ was converted to $^{237}U$ by the end of the irradiation. The target also contained curie quantities of $^{238}Np$, $^{239}Np$, $^{24}Na$, and fission products, and also significant quantities of $^{237}Np$ and $^{51}Cr$.

### B. Chemical purification

Because of the high radiation levels involved, dissolution of the HFIR target, purification of the uranium, and preparation of the isotope separator charge material had to be carried out in hot cells. The center of the rabbit, containing about 5 g of aluminum in addition to the uranium, was dissolved in a HCl-$HNO_3$ mixture. The major steps in the chemical purification procedure involved adsorption of the uranium from a large volume of HCl (8–9 $M$) onto an ion exchange resin column, extraction of the stripped uranium into ethyl acetate from an $HNO_3$-$Al(NO_3)_3$ solution, and a second adsorption of the back-extracted uranium onto an

TABLE I. Target composition.

| Nucleus | Amount |
|---|---|
| $^{237}U$ | $18.1 \pm 0.5$ $\mu g$ |
| $^{237}Np$ | $6.9 \pm 0.1$ $\mu g$ |
| $^{236}U$ | $0.5 \pm 0.05$ $\mu g$ |
| $^{238}Np$ | $2.9 \times 10^{10}$ atoms |

ion exchange resin column. Washing of the second column with HCl-HI and HCl-HF solutions provided the important decontamination from $^{237}Np$. Further details of the chemical procedure are given in Ref. 5.

### C. Isotopic separation and target preparation

The chemically purified uranium, in a concentrated solution, was transferred to a quartz wool wad in a quartz tube, evaporated to dryness, and converted to $U_3O_8$ by heating to ~800°C in air. This oxide constituted the charge material that was inserted into the ion source of the LASL electromagnetic isotope separator.[6] By means of the standard internal chlorination technique,[7] using $CCl_4$, ion beams of the uranium isotopes were produced and then accelerated to 50 keV. While the 5- to 10-$\mu$A $^{236}U^+$ beam was monitored with a simple collector cup and electrometer, the adjacent $^{237}U$ beam passed through the entrance slit of a retardation lens[8] to reduce the ion energy to about 300 eV to prevent sputtering. The $^{237}U$ was deposited on the center of a 2.5-$\mu$m-thick, 5-cm-diam stainless-steel foil. The buildup of the $^{237}U$ deposit was monitored with a highly directional NaI(Tl) scintillator set to count the 0.332-MeV $\gamma$ ray following decay of $^{237}U$. Three separate uranium charges, totaling about 34 mg of $^{236}U$ and about 50 ci of $^{237}U$, were processed through the isotope separator over a 40-h period to provide the final $^{237}U$ target for the Pommard event. The deposit covered an area of ~1 cm$^2$ lying totally within the area through which the collimated neutron beam passed.

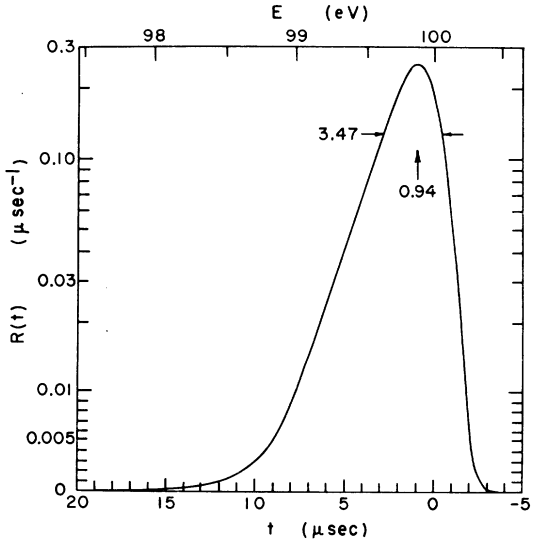


FIG. 1. Resolution function $R(t)$ plotted vs time with energies indicated for a resonance at 100 eV. Note that the ordinate scale is logarithmic above and linear below 0.01, with continuous first derivative.

### D. Composition of the target

The $^{237}U$ content of the target deposit was determined in a number of ways. Direct measurement of the $^{237}U$ was made before and after the experiment by means of a precalibrated Ge(Li) detector. Because of the high activity level, the target foil was placed in a lead cell 6.4 cm from the detector and the 332.4-keV $\gamma$ rays were counted through 1.84 cm of lead. After the Pommard event, the uranium deposit was dissolved from the foil. The $^{237}U$ was then determined on a small, precisely measured aliquot by a standard radiochemical procedure involving the measurement of the disintegration rate with a calibrated $\beta$ proportional counter. The three determinations were in good agreement. Analyses were also made for $^{237}Np$ and $^{238}Np$ to determine their concentration in the target deposit at the time of the Pommard event. Traced mass-spectrographic analyses gave the $^{236}U/^{237}U$ ratio. The values obtained for the composition of the target deposit at the time of the event are given in Table I.

### E. Half-life of $^{237}U$

The solution obtained from the dissolution of the target deposit provided excellent sources for an

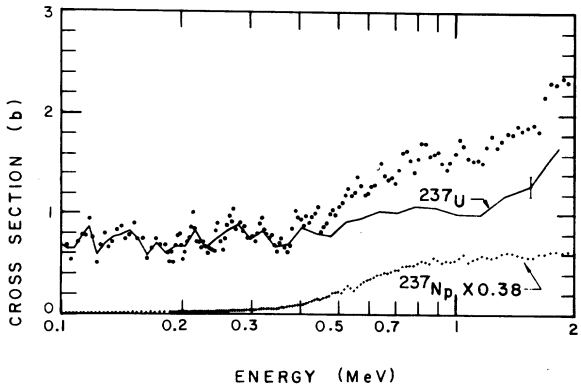


FIG. 2. $^{237}U$ fission cross section, 0.1–2 MeV. The line is the average of detectors at 55 and 90° after subtraction of the $^{237}Np$ contaminant.

accurate determination of the half-life of $^{237}U$. The $\beta$-disintegration rates of overlapping and progressively larger aliquots from the same $^{237}U$ solution were measured over a period of 230 days, covering the decay from $3.2\times10^9$ counts/min to a long-lived residue of 35 counts/min, due to the $^{233}Pa$ granddaughter. The resulting half-life[9] is $6.7\pm0.02$ days.

## III. EXPERIMENTAL MEASUREMENTS

The $^{237}U$ target foil was placed 214.23 m from the center of the nuclear device, or 213.82 m from the near face of the moderator. In the same neutron beam, there was a $^6Li$ target at 214.43 m, a $^{235}U$ target at 214.63 m, a blank 2.5-$\mu$m backing foil at 214.83 m, and a $^{237}Np$ target at 215.24 m from the moderator, as well as other fission samples to be measured. An adjacent beam included a $^{238}Pu$ target,[10] used to measure resolution.

### A. Resolution

The radiations reaching the target include a large pulse of electromagnetic energy at 0.715 $\mu$sec after the explosion, direct fission neutrons, single-scattered neutrons from the hydrogenous high-explosive material surrounding the device (at a temperature of about 1–3 keV) and from the moderator, and the neutrons trapped in the moderator and reemitted when the moderator is heated, squeezed, and accelerated by the explosion shock wave. Thus, the source resolution function varies with neutron energy, from a 0.1-$\mu$sec pulse for energies above 100 keV to the moderator emission function, which dominates below 300 eV. This function was fitted by a Gaussian folded with an exponential tail, with the two free parameters adjusted to six narrow resonances[11] in $^{238}Pu$ between 80 and 200 eV, taking account of natural and Doppler widths. The result is shown in Fig. 1, plotted vs $t$ and also vs $E$ for $E_0=100$ eV. The net full width at half maximum is 3.47 $\mu$sec.

### B. Background

The principal source of background was an exponentially decaying component following the initial electromagnetic flash. This could be from ionization of the residual gas in the target vacuum chamber. Because the $^{237}U$ sample was very small, the background subtraction amounted to 20% at 1 MeV and 50% at 100 keV.

An instrumental malfunction at 50 $\mu$sec after the neutron burst caused all data to be lost for 250 $\mu$sec and shifted the amplifier base lines. Thus, an arbitrary shift of $0.06\pm0.03$ mV was subtracted to make the signal as small as possible at late times when the flux had diminished to nothing, without going very negative between resonances at 60 eV. This results (for instance) in a 20% uncertainty in the valley at 100 eV. For larger signals the amplifier had a logarithmic characteristic; thus the shift produced a 1% systematic uncertainty.

TABLE II. Assumed cross section for $^{235}U(n,f)$ at 55°.

| $E$ (MeV) | $\sigma$ (b) | $E$ (MeV) | $\sigma$ (b) |
|---|---|---|---|
| 0.091 | 1.65 | 0.783 | 1.15 |
| 0.101 | 1.63 | 0.821 | 1.18 |
| 0.150 | 1.50 | 0.907 | 1.21 |
| 0.202 | 1.41 | 1.000 | 1.22 |
| 0.302 | 1.29 | 1.11 | 1.22 |
| 0.408 | 1.22 | 1.22 | 1.22 |
| 0.450 | 1.19 | 1.35 | 1.22 |
| 0.498 | 1.17 | 1.50 | 1.23 |
| 0.550 | 1.15 | 1.65 | 1.25 |
| 0.608 | 1.14 | 1.83 | 1.28 |
| 0.672 | 1.13 | 2.02 | 1.31 |

### C. Flux

As the signal and flux detectors were in nominally identical geometry and the relative efficiencies were measured, the experimental measurements may be considered as ratios to the known cross sections for $^6Li(n,\alpha t)$ and $^{235}U(n,f)$. The data from 40 eV to 1 keV were normalized to a $1/v$ dependence cross section for $^6Li(n,\alpha t)$ with $\sigma(2200\ \text{m/sec})=940.3\pm1.6$ b. Above $10^5$ eV, the $^{235}U(n,f)$ evaluation by Davey[12] was modified for angular correlation to give the 55° data of Table II; any changes in this cross section would change our reported values proportionally. An uncertainty of 4% was assigned to these values. A complete discussion of flux determination and data reduction is given in a LASL report.[4]

### D. Data

Data from two solid-state detectors of solid angles 0.1806 and 0.0743 sr at 55 and 90°, respectively, were averaged for the high-energy region, while only the 90° detector was used at low energies. The high-energy data are shown in Fig. 2, which indicates the subtraction of the $^{237}Np$ contribution as measured[13] simultaneously. No other contaminant corrections were necessary. Both detectors indicate the rise between 1–2 MeV; the signal from the 90° detector, with a smaller background correction, is roughly constant from 2–3 MeV.

The data are tabulated in a LASL report[14]; uncertainties included there and also on the error

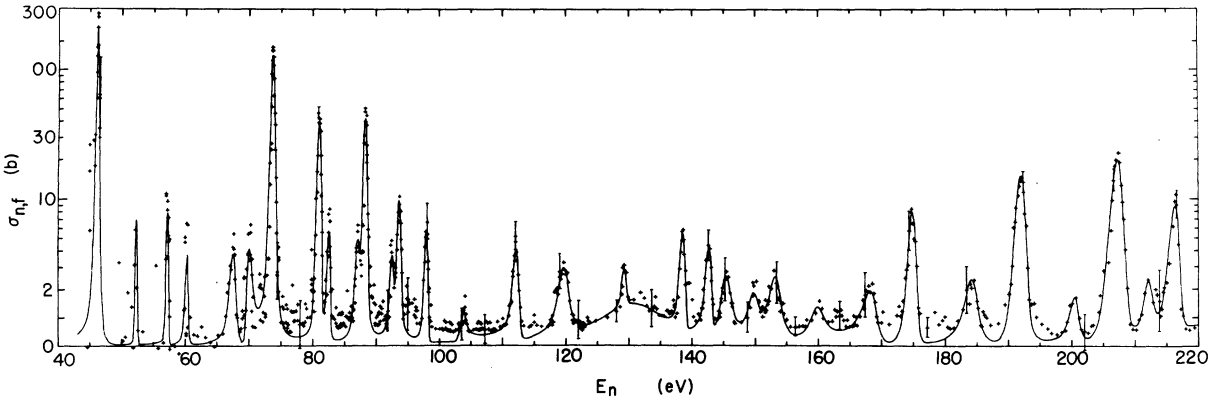


FIG. 3. $^{237}$U fission cross section, 43–220 eV, with fitted multilevel curve. Error bars on points include 6% systematic uncertainty. The ordinate scale is logarithmic above and linear below 2 b, with continuous first derivative. Such a scale allows both peaks and valleys to be seen, and matches the gain characteristic of the amplifiers used.

bars of Figs. 2–4 include statistical errors based on counting rates and random errors arising in the data reduction, as well as systematic uncertainties, listed in Table III. (Errors given are standard deviations.) Before any manipulations are done involving errors (e.g., weighted averaging or finding the error of an integral), the systematic uncertainty must be removed quadratically, and recombined with the result.

## IV. ANALYSIS AND COMPARISON

### A. 0.1-2 MeV

Estimation of the 3-MeV cross section from systematics[15] gives 0.7 b, which does not agree with the rise we see above 1 MeV, but does agree with the observed level from 0.1–0.5 MeV. The cross section was measured in 1954 at this laboratory[16] with two different neutron sources; each peaked near 200 keV. The results were $0.66 \pm 0.10$ and $0.70 \pm 0.07$ b, in good agreement with the current experiment. However, when the sample used in this experiment was compared to $^{235}$U in a critical assembly measurement,[17] the cross-section ratio was $0.391 \pm 0.012$; summing our results over the assumed neutron spectrum of the assembly gives $\sigma(237)/\sigma(235) \approx 0.62$.

TABLE III. Sources of systematic uncertainty.

| | 43–1000 eV (%) | 0.1–2 MeV (%) |
|---|---|---|
| Target density | 3.0 | 3.0 |
| Detector geometry | 1.6 | 1.2 |
| Reference | 0.2 | 4.0 |
| Flux determination | 2.9 | 2.6 |
| Fragment energy | 3.4 | 3.1 |
| Base line | 1.0 | ··· |
| Amplifier input $R$ | 1.0 | 0.7 |
| Total | 5.8% | 6.6% |

### B. 43-1000 eV

A fit of resonance parameters was made between 43 and 220 eV. A multilevel analysis was performed with the program MULTI,[18] which makes a least-squares adjustment to $R$-matrix parameters; however, the fitting was greatly hampered by the poor quality of the data in the valleys, which prevented accurate determination of interference, and by the lack of a corresponding total absorption or scattering measurement, which makes independent estimations of both neutron and fission widths difficult. $\gamma$ width was assumed constant at 35 meV. The resulting fitted curve is shown as a line in

TABLE IV. Fitted resonance areas. Uncertainties are based on integrals of the data.

| $E_0$ (eV) | $\frac{1}{2}\pi\sigma_0\Gamma_f$ (b eV) | $E_0$ (eV) | $\frac{1}{2}\pi\sigma_0\Gamma_f$ (b eV) |
|---|---|---|---|
| 46.2 | 84. ±14. | 129.5 | 1.5±0.2 |
| 52.4 | 3.0± 2.6 | 131 | 29 |
| 57.3 | 4.2± 1.8 | 138.8 | 5.8±0.6 |
| 60.3 | 2.5± 1.4 | 143.0 | 5.2±0.6 |
| 67.5 | 6.4± 1.5 | 145.4 | 5.9±0.8 |
| 70.0 | 4.3± 0.8 | 149.9 | 4.0±0.7 |
| 73.8 | 83.4± 5.7 | 153.7 | 6.8±0.9 |
| 81.1 | 26.1± 1.9 | 160.2 | 4.4±0.8 |
| 82.7 | 3.4± 0.4 | 169.1 | 5.8±0.8 |
| 87.3 | 5.0± 0.5 | 175.3 | 11.9±1.3 |
| 88.4 | 29.7± 2.3 | 184.9 | 8.0±1.3 |
| 92.7 | 3.1± 0.5 | 192.4 | 27.3±2.7 |
| 93.7 | 7.9± 0.8 | 200.9 | 3.4±0.7 |
| 98.0 | 4.2± 0.5 | 207.7 | 40.8±3.4 |
| 103.9 | 1.2± 0.2 | 212.4 | 4.3±0.8 |
| 112.4 | 5.3± 0.6 | 216.7 | 15.9±1.8 |
| 119.9 | 7.2± 0.8 | 235 | 64 |

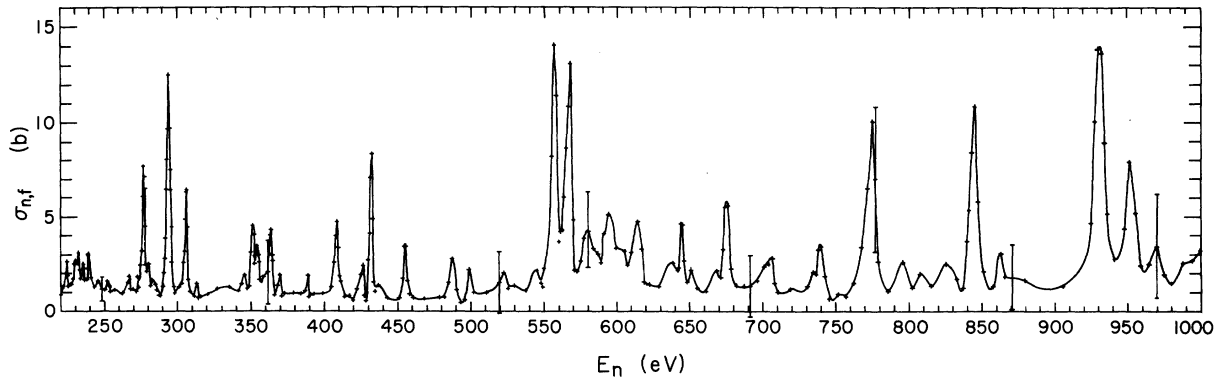


FIG. 4. $^{237}U$ fission cross section, 220–1000 eV. The line is a smooth (spline) curve joining all data points, as a reminder that the data were originally recorded in analog form as an oscillograph trace. Signal levels were low in this energy range, remaining within the linear portion of the amplifier characteristic.

Fig. 3. The statistics of the measurement were very poor, and the source resolution function was too wide to permit accurate shape analysis; therefore, only the areas of the fitted resonances are given in Table IV. It should be noted that no correction has been made for the $\gamma$ sensitivity of the fission detectors. Comparison with a similar experiment[19] on $^{244}Cm$, however, indicates the correction is about 0.3% of $\frac{1}{2}\pi\sigma_0\Gamma_f$ on the average, and hence negligible.

The level spacing of the observed fission resonances was estimated as $3.5 \pm 0.8$ eV, from the relatively well-determined resonances between 65 and 100 eV. Comparing this to $^{239}Pu$ by using, for example, the Gilbert and Cameron formula[20] (which includes corrections for $Z, A$, and excitation differences) suggests that both $0^+$ and $1^+$ resonances are observed.

The average cross section over selected energy intervals is given in Table V; the average from 300 to 1000 eV is just 30% of that for $^{239}Pu$. If both channels ($0^+$ and $1^+$) are open, as suggested by the observed level spacing, then the measured average cross section is extremely low. From fitting a measurement[21] of $^{236}U(t, pf)$, Back *et al.*[22] suggest that the $0^+$ threshold of $^{237}U(n, f)$ appears to be approximately at neutron binding. Therefore, the $1^+$ threshold is well above neutron binding, and the observed $1^+$ levels must be attributed to some mechanism which does not contribute appreciably to the average cross section. If we tentatively assign the largest of the fission resonances in Table IV to the $0^+$ spin state and estimate the average fission width of the rest under the assumption that $\langle\Gamma_n^0\rangle/D = 1\times10^{-4}$, we find that $\langle\Gamma_f\rangle_{1^+} \simeq 0.8$ meV. This is consistent with recent results of Frehaut and Shackleton,[23] who estimate the average width for the $(n,\gamma f)$ process in ($^{239}Pu + n$) as ~1 meV. The average cross section between 300 and 1000 eV is then consistent with purely $0^+$ fission, with an average width of ~500 meV. Thus our results are not inconsistent with systematics.

TABLE V. Average fission cross section.

| $\Delta E$ (eV) | $\bar{\sigma}$ (b) | $\Delta E$ (eV) | $\bar{\sigma}$ (b) |
|---|---|---|---|
| 43–65 | 3.89 ± 0.93 | 500–600 | 3.31 ± 0.35 |
| 65–100 | 5.06 ± 0.32 | 600–700 | 2.27 ± 0.30 |
| 100–200 | 1.52 ± 0.10 | 700–800 | 2.18 ± 0.33 |
| 200–300 | 2.29 ± 0.16 | 800–900 | 2.27 ± 0.34 |
| 300–400 | 1.51 ± 0.15 | 900–1000 | 4.02 ± 0.54 |
| 400–500 | 1.37 ± 0.20 | | |

Special attention is called to resonances at 131 and 235 eV with fitted fission widths of 13 and 23 eV, respectively. These were necessary to obtain a satisfactory fit. When an additonal wide level was assumed near 80 eV, however, the MULTI program "rejected" it by moving it out of range. From a study of Fig. 4 and other plots[14] of the data, other such features may exist at 580 and 950 eV; these may point to the existence of resonance effects in the second well, similar to those observed[19,20] in the $^{236}U(t, pf)$ work at effective neutron energies of −340 and −1000 keV.

## ACKNOWLEDGMENTS

The authors would like to thank R. Baybarz and J. Bigelow (ORNL) for fabricating the HFIR rabbit and for all arrangements involving the HFIR irradiation. We acknowledge the analysis of the $^{237}U$ target deposit performed by H. L. Smith and D. W. Barr (LASL) and the assistance of G. M. Kelley (LASL) in operating the isotope separator. We thank D. K. Ferguson, G. A. Cowan, B. C.

Diven, and A. Hemmendinger (LASL) for encouragement in this project, as well as the large number of people in the LASL testing division whose commitment "above and beyond the call of duty" is so essential to the success of such a complex field operation. M. S. Moore and J. A. Farrell have been very helpful in the analysis of results.

---

[1]P. A. Seeger, A. Hemmendinger, and B. C. Diven, Nucl. Phys. A96, 605 (1967).
[2]D. W. Bergen and R. R. Fullwood, Nucl. Phys. A163, 577 (1971).
[3]A. Hemmendinger, B. C. Diven, W. K. Brown, A. Ellis, A. Furnish, E. R. Shunk, and R. R. Fullwood, Los Alamos Scientific Laboratory Report No. LA-3478, 1968 (unpublished), Part I; P. A. Seeger and D. W. Bergen, Los Alamos Scientific Laboratory Report No. LA-3478, 1967 (unpublished), Part II.
[4]W. K. Brown, P. A. Seeger, and M. G. Silbert, Los Alamos Scientific Laboratory Report No. LA-4095, 1970 (unpublished).
[5]K. Wolfsberg, Los Alamos Scientific Laboratory Report No. LA-1721 (unpublished), 3rd ed., revised 1969, p. 156a.
[6]The LASL isotope separator is an improved version of the Stockholm separator described by T. Alväger and J. Uhler in Ark. Fys. 13, 145 (1957). It was obtained from the Nuclear Engineering and Equipment Company (Nuclesa) of Geneva, Switzerland.
[7]G. Sidenius and O. Skilbreid, in *Electromagnetic Separation of Radioactive Isotopes*, edited by M. J. Higatsberger and F. P. Viehboch (Springer-Verlag, Vienna, 1961), p. 243.
[8]J. Uhler, Ark. Fys. 24, 349 (1963).
[9]H. L. Smith, private communication.
[10]D. M. Drake, C. D. Bowman, M. S. Coops, and R. W. Hoff, to be published (see also Ref. 14).
[11]M. G. Silbert, A. Moat, and T. E. Young, Nucl. Sci. Eng. 52, 176 (1973).
[12]W. G. Davey, Nucl. Sci. Eng. 32, 35 (1968).
[13]W. K. Brown, D. R. Dixon, and D. M. Drake, Nucl. Phys. A156, 609 (1970).
[14]Los Alamos Scientific Laboratory Report No. LA-4420, 1970 (unpublished), p. 91.
[15]R. L. Henkel and H. H. Barschall, as quoted by E. K. Hyde, *The Nuclear Properties of the Heavy Elements*, (Prentice-Hall, New Jersey, 1964), Vol. III, p. 73.
[16]G. A. Cowan *et al.*, Los Alamos Scientific Laboratory Report No. LA-1669, 1955 (unpublished).
[17]D. W. Barr, private communication.
[18]G. F. Auchampaugh, Los Alamos Scientific Laboratory Report No. LA-4633, 1974 (unpublished).
[19]M. S. Moore and G. A. Keyworth, Phys. Rev. C 3, 1656 (1971).
[20]A. Gilbert and A. G. W. Cameron, Can. J. Phys. 43, 1446 (1965).
[21]J. D. Cramer and H. C. Britt, Nucl.Sci.Eng. 41, 177(1970)
[22]B. B. Back, Ole Hansen, H. C. Britt, and J. D. Garrett, in *Third IAEA Symposium on the Physics and Chemistry of Fission, Rochester, 13–17 August 1973* (International Atomic Energy Agency, Vienna, 1973), paper IAEA/SM-174/27 and unpublished.
[23]J. Frehaut and D. Shackleton, in *Physics and Chemistry of Fission* (see Ref. 22), paper IAEA/SM-174/47.